Molecular Biology of the Cell
Vol. 7, 471–482, March 1996

Membrane Integration of In Vitro–translated Gap Junctional Proteins: Co- and Post-translational Mechanisms

Jian-Ting Zhang,* Mingang Chen,* Cynthia I. Foote, and Bruce J. Nicholson†

Department of Biological Sciences, State University of New York at Buffalo, Buffalo, New York 14260-1300

Submitted September 15, 1995; Accepted December 8, 1995
Monitoring Editor: Ari Helenius

Connexins (Cx) are protein components of gap junction channels that permit the passage of small molecules between neighboring cells. cDNAs of a large family of connexins have been isolated and sequenced. A gap junction channel consists of two connexons, one from each cell in contact, composed of six connexin subunits. It has been suggested by Musil and coworkers that the oligomerization or formation of a connexon occurs at the level of the *trans*-Golgi network. In the present study, we initiated an analysis of the early stages of protein synthesis and membrane insertion of Cx32 and Cx26, two connexins that we have demonstrated are co-expressed in the same junctions in hepatocytes. Using an in vitro transcription and a coupled cell-free translation and translocation system, we observed that both Cx32 and Cx26 could insert into microsome membranes co-translationally, producing a topological structure indistinguishable from that in isolated gap junctions. To our surprise, Cx26 could also insert into membranes post-translationally with a native orientation. This post-translational membrane insertion process is dependent on nucleotides but not their hydrolysis. Cx32, on the other hand, could not insert into membranes post-translationally. These disparate properties of Cx32 and Cx26 are not due to the significant difference in the lengths of their C-terminal domains, but rather to their internal amino acid sequences. These observations raise the possibility that there may be another pathway for Cx26 to insert into membranes in cells and this feature may be important for the regulation of its functions. These findings may also lead us to a new approach to reconstitution without detergent extraction.

INTRODUCTION

Gap junctions are specialized regions of plasma membranes comprised of closely packed complexes of channels that pass small molecules between cells in contact (Bennett and Goodenough, 1978; Loewenstein, 1979). It has been suggested, from a variety of systems, that gap junctionally mediated communication plays an essential role in the coordination of contraction in smooth and cardiac muscle (Spray and Burt, 1990), formation of electrical synapses that couple some neurons (Yang *et al.*, 1990), and regulation of cell proliferation and differentiation (Loewenstein, 1979; Sheridan and Atkinson, 1985; also see reviews by Klaunig and Ruch, 1990 and by Guthrie and Gilula, 1989).

Oligomerization of six gap junction protein subunits (termed connexins or Cx) generate a connexon. Two connexons, one from each neighboring cell, interact and form a functional gap junction channel. A large family of gap junction proteins have now been described and cloned (for a review see Kumar and Gilula, 1992). The hydropathy plot analyses of the deduced amino acid sequences suggest that gap junction proteins span the membrane four times. Topological

* Current address: Department of Physiology and Biophysics, University of Texas Medical Branch, Galveston, Texas 77555-0641.
† Corresponding author.

mapping of three of these connexins using peptide-specific antibodies and proteolysis has confirmed this model and shown that both the N- and C-terminal ends of connexins are disposed cytoplasmically (Nicholson *et al.*, 1981; Hertzberg *et al.*, 1988; Milks *et al.*, 1988; Yancey *et al.*, 1989; Rahman and Evans, 1991; Zhang and Nicholson, 1994). Gap junction proteins belong to the class of polytopic type IV plasma membrane proteins (see von Heijne and Gavel, 1988 for classification).

More than other membrane channels, biosynthesis of gap junctions represents a complex, multistep process that must include not only oligomerization of the connexins and their transport to the cell surface, but also docking of connexons from adjacent cells and the lateral aggregation of channels. Musil and Goodenough (1993) concluded that oligomeric assemblies first form at a very late stage in the *trans*-Golgi network. In this study, we focused on earlier stages of connexin synthesis: the membrane insertion process. We employed an in vitro transcription and coupled cell-free translation and translocation system. The cell-free systems are easy to manipulate, and provide a means to examine the early stages of the assembly process. The generally used cell-free systems are rabbit reticulocyte lysate and wheat germ extract supplemented with dog pancreatic rough microsome membranes (RM) (Jagus, 1987). These systems have been widely used to identify export and membrane insertion machineries, including the signal recognition particle (SRP) (Walter and Blobel, 1980), its receptor (Gilmore *et al.*, 1982; Meyer *et al.*, 1982), and the signal peptidase (Evans *et al.*, 1986). These systems are also useful for determining the topological orientation of membrane proteins (Andrews, 1989; Zhang and Ling, 1991), and in identifying and examining the amino acid sequences that specify membrane protein topology (Rothman *et al.*, 1988; Zhang *et al.*, 1995). This general approach was also applied to gap junction proteins by Falk *et al.* (1994) while the current research was in progress. However, in these studies, the topology of the proteins within the membranes was inconsistent with that seen in isolated gap junctions. Furthermore, apparent cryptic cleavage by signal peptidase not seen in vivo, except under conditions of overexpression, was seen with several different connexins.

The current study aims to fully characterize the rabbit reticulocyte lysate translation and translocation system to examine the early stages of protein synthesis and membrane insertion of Cx32 and Cx26, two closely related connexins that are expressed in hepatocytes in the same junctional structures (Nicholson *et al.*, 1987). We observed that both the newly synthesized Cx32 and Cx26 can co-translationally insert into microsome membranes with the same orientation as connexins in intact gap junctional plaques (Zhang and Nicholson, 1994), although the same partial cleavage at a cryptic signal sequence site reported by Falk *et al.* (1994) is seen. Surprisingly, Cx26 was also found to be able to insert into microsome membranes post-translationally in a ribonucleotide triphosphate–dependent manner. The post-translationally inserted Cx26 also has a membrane orientation indistinguishable from Cx26 in situ. However, Cx32, like virtually all other higher eukaryotic plasma membrane proteins, does not insert into membranes post-translationally. Our studies using chimeric proteins of Cx32 and Cx26 showed that this difference between Cx26 and Cx32 is not due to the length of the C-terminal tail of the proteins (i.e., net hydrophobicity), but rather is determined by the internal amino acid sequences.

MATERIALS AND METHODS

In Vitro Transcription and Translation

About 4 μg of pGEM-4Z vector containing Cx32 or pGEM-3Z with Cx26 were linearized with *Hin*dIII and *Eco*RI, respectively, and transcribed with SP6 RNA polymerase in a 100-μl reaction mixture (using a kit from Promega, Madison, WI) in the presence of 5 A_{260} units of cap analogue (m7G(5′)ppp(5′)G). RNA transcripts were purified by removing the DNA template with RQ1 DNase digestion, phenol/chloroform and chloroform extraction, and ethanol precipitation according to the protocols provided by Promega. RNA from each reaction was dissolved in 13 μl diethylpyrocarbonate-treated H_2O containing 1 U/μl RNasin (Promega). The yield of RNA was typically 20 μg per reaction estimated by OD_{260}. Translation of 60 ng/μl of RNA in 50 μl rabbit reticulocyte lysate in the presence or absence of RM (Amersham, Arlington Heights, IL, or Promega) occurred over 90 min at 30°C in the presence of 1 μCi/μl [^{35}S]methionine (NEN, Boston, MA). For post-translational membrane insertion, translation was performed in the absence of RM. The RNA templates were then removed by RNase A digestion (30°C, 10 min). To confirm the effectiveness of this treatment, some samples were also treated with puromycin. RM were then added to the resulting mixture and incubated at 30°C for 90 min before analysis by SDS-PAGE. To determine the co-factor requirement for the post-translational membrane insertion of Cx26, low molecular weight components in the lysates were removed after RNase A digestion by separation using two successive 0.9-ml Sephadex G-25 spin columns that were pre-equilibrated with 50 mM Tris, pH 7.5, 5% glycerol, 0.1 M KAc, 5 mM $Mg(Ac)_2$, 2 mM dithiothreitol, and 1% bovine serum albumin (BSA). The void volume eluate was then divided into aliquots and supplemented with various concentrations of ATP, UTP, CTP, GTP, AMP-PCP, ATP-γS, PPi, AMP, or ADP. RM were then added, followed by incubation at 30°C for 90 min before analysis by SDS-PAGE.

In both co- and post-translational experiments, microsomes were washed by dilution into 1 ml of ice cold 0.1 M Na_2CO_3 (pH 11.5). Following a 15-min incubation on ice, microsomes were either pelleted directly or through a cushion of 250 mM sucrose in 500 mM K acetate, 5 mM Mg acetate, and 50 mM *N*-2-hydroxyethylpiperazine-*N*′-2-ethanesulfonic acid (HEPES) (pH 7.9). Initially, centrifugation for 30 min in a microfuge was used. In later experiments, yields were increased by centrifugation in a TLA rotor in a Beckman microfuge (Fullerton, CA) for 10 min at 150,000 × *g*.

Proteolysis/Membrane Protection Assay

Microsomes containing newly synthesized Cx32 or Cx26 were pelleted by centrifugation, resuspended in STBS buffer (0.25 M sucrose, 10 mM Tris/HCl, pH 7.5, 150 mM NaCl), and then subjected to digestion by pronase, trypsin, or protease V8. The proteolysis reac-

tion was carried out on ice for 30 min, and terminated by adding 1 μg/ul soybean trypsin inhibitor (Sigma, St. Louis, MO) or phenylmethylsulfonyl fluoride (Sigma) to a final concentration of 2 mM. RM membranes with membrane-protected nascent protein fragments were collected by centrifugation (15,000 × *g* for 15 min) before analysis by SDS-PAGE. Proteolysis/membrane protection and Western blot analyses of isolated gap junctions were performed as described previously by Zhang and Nicholson (1994).

Immunoprecipitation and Absorption

After stopping the proteolysis of RM fractions with protease inhibitor and removing soluble protease by centrifugation, the membrane pellet was solubilized in an immunoprecipitation buffer (1% Triton X-100, 10 mM Tris, pH 7.4, 0.9% NaCl). Polyclonal antisera to different domains of Cx32 and Cx26 (see Figure 4) were added at 1/100 dilutions to the mixture and incubated overnight at 4°C. Protein A-Sepharose beads were then added to the mixtures to a final concentration of 0.4 mg/ml, followed by incubation at room temperature with shaking for 1.5 h. The protein A-Sepharose fraction was then pelleted and washed four times with the immunoprecipitation buffer containing 0.2% BSA before analysis by SDS-PAGE.

To study the membrane disposition of translated proteins in the membrane, immuno-absorption was performed. RM fractions of a translation mixture were pelleted, resuspended in phosphate-buffered saline (PBS) at pH 7.4, and divided into two halves. One-half was sonicated in the presence of 1% Triton X-100 whereas the other was untreated. Both the sonicated and untreated RM fractions were then subjected to immuno-absorption using nitrocellulose discs bound with Cx32- or Cx26-specific polyclonal antibodies directed against peptide epitopes in both their extracellular and intracellular domains (Zhang and Nicholson, 1994). These discs (6 mm in diameter) were prepared by incubation in 50 μg/ml protein A in PBS for 2 h at room temperature, followed by five washes in PBS, a second incubation in either preimmune or immune serum to Cx32 or Cx26 for 1.5 h at 37°C, and final blocking in 3% BSA in PBS before five washes in PBS. Finally, the nitrocellulose discs were used to absorb both untreated or sonicated RM by overnight incubation with shaking at room temperature. After five washes in PBS, the nitrocellulose discs were prepared for scintillation counting.

SDS-PAGE Analysis

SDS-PAGE was performed according to the method of Laemmli (1970). After electrophoresis, the gels were fixed in dimethyl sulfoxide, treated with PPO, dried, and exposed to Kodak XAR-5 film (Rochester, NY) at −70°C from a few hours to a few days for fluorography.

Site-directed Mutagenesis and Chimera Construction

The 1.5-kb Cx32 cDNA (Paul, 1986) and the 1.1-kb Cx26 cDNA (Zhang and Nicholson, 1989) were cloned into pGEM7Zf+ (Promega) at the *Eco*RI site. Orientation of the inserts was selected such that the SP6 promoter would produce a sense transcript of Cx32 and the T7 promoter would produce a Cx26 sense transcript. Mutants were made by the method of Kunkel *et al.* (1987). Glutamine 222 of Cx32 was changed to the TAG stop codon with the mutagenic oligonucleotide 5′CGGCGCTAAGCACGGC3′, producing the Cx32 Q_{222}TAG mutant. To create a chimera of Cx26 with the carboxyl-tail of Cx32 ($Cx26_{1-199}/Cx32_{200-283}$), a silent *Acc*III site was introduced at the same position in both Cx26 and 32 sequences using the oligonucleotides: $5'_{610}$GGATGCAAATTCCGGACACAG$_{590}3'$ and $5'_{610}$GGATAATGCAGATTCCGGAGG$_{590}3'$, respectively. Cutting with *Acc*III and ligation produced the desired chimera. All constructs were checked by sequencing. Transcriptions and translations were carried out as described above, or using the TNT-coupled reticulocyte system of Promega.

RESULTS

In Vitro Transcription and Translation of Cx32 and Cx26

To study and compare the protein synthesis and membrane insertion of Cx32 and Cx26, we expressed these proteins using an in vitro transcription and a coupled cell-free translation and translocation system. Figure 1A shows rat Cx32 and Cx26 cDNA constructs containing the entire coding regions cloned in pGEM expression vectors. The run-off sense and antisense strand RNA transcripts were synthesized using SP6 RNA polymerase from constructs with different orientations of cDNA inserts in the presence of [α-^{32}P]UTP. The ^{7}mGpppG-capped transcripts were treated with glyoxal and separated by electrophoresis in a 1% agarose gel (Figure 1C). Both sense (Figure 1C, lane 3) and antisense (Figure 1C, lane 4) transcriptions of Cx32 cDNA linearized with *Hin*dIII generated a single product of ~1.6 kb. Sense transcription of Cx26 cDNA linearized with *Eco*RI (Figure 1C, lane 1) produced two products of 1.1 kb and 0.9 kb whereas the antisense transcription (Figure 1C, lane 2) gave a single product of 1.1 kb. The 1.1-kb transcripts of Cx26 (Figure 1C, lanes 1 and 2) represent the full-length sense and antisense RNA products whereas the 0.9-kb product (Figure 1C, lane 1) apparently results from the premature termination of the sense transcript due to the presence of a stem-loop structure predicted to form at this site (Figure 1, A and B). Consistent with this possibility is the observation that transcription of Cx26 cDNA linearized with *Bst*XI, which cuts to the 5′ side of this potential stem-loop structure, produced only one RNA product. Unfortunately, since this truncated RNA does not include the full coding region of Cx26, subsequent translation studies used the mixture of 1.1- and 0.9-kb transcripts.

Figure 1D shows the primary translation products of Cx32 and Cx26 in rabbit reticulocyte lysate. Cx32 sense strand RNA transcripts directed translation of a 29-kDa protein (Figure 1D, lane 3), equivalent to the size of isolated Cx32, whereas the antisense strand RNA produced no protein products (Figure 1D, lane 4). Translation of Cx26 sense RNA transcripts produced a major product of ~25 kDa (Figure 1D, lane 1) while control reaction with the antisense Cx26 RNA did not generate any proteins. The 43-kDa protein (Figure 1D, lane 1) is likely an aggregated dimer of the 25-kDa protein, consistent with previous studies where aggregation of Cx32 and Cx26 has been observed (Nicholson *et al.*, 1981). The 25-kDa protein is consistent with the production of native Cx26 from the full-length 1.1-kb transcript. The minor, poorly resolved components below the 25-kDa protein (indicated by arrowhead

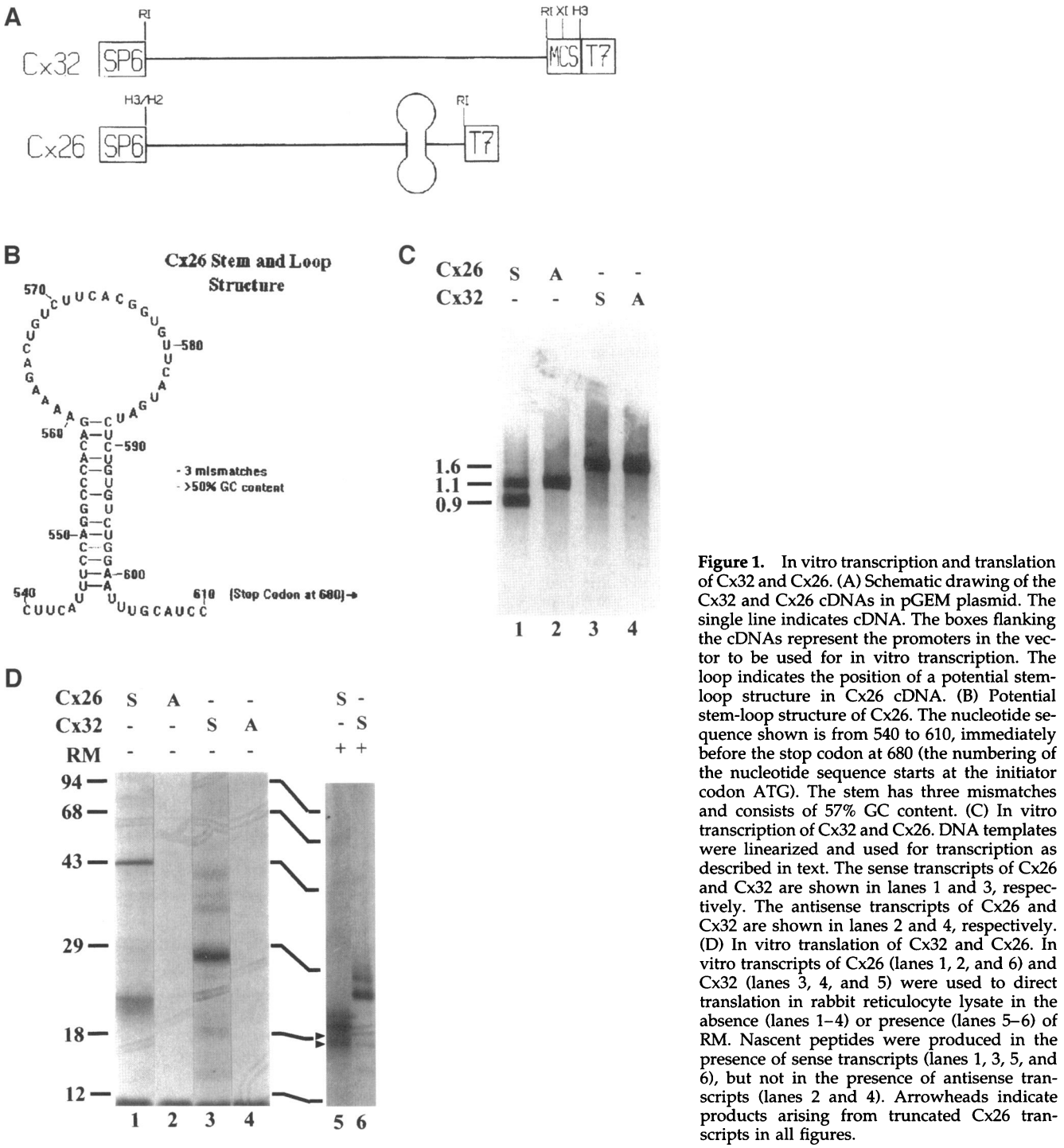

Figure 1. In vitro transcription and translation of Cx32 and Cx26. (A) Schematic drawing of the Cx32 and Cx26 cDNAs in pGEM plasmid. The single line indicates cDNA. The boxes flanking the cDNAs represent the promoters in the vector to be used for in vitro transcription. The loop indicates the position of a potential stem-loop structure in Cx26 cDNA. (B) Potential stem-loop structure of Cx26. The nucleotide sequence shown is from 540 to 610, immediately before the stop codon at 680 (the numbering of the nucleotide sequence starts at the initiator codon ATG). The stem has three mismatches and consists of 57% GC content. (C) In vitro transcription of Cx32 and Cx26. DNA templates were linearized and used for transcription as described in text. The sense transcripts of Cx26 and Cx32 are shown in lanes 1 and 3, respectively. The antisense transcripts of Cx26 and Cx32 are shown in lanes 2 and 4, respectively. (D) In vitro translation of Cx32 and Cx26. In vitro transcripts of Cx26 (lanes 1, 2, and 6) and Cx32 (lanes 3, 4, and 5) were used to direct translation in rabbit reticulocyte lysate in the absence (lanes 1–4) or presence (lanes 5–6) of RM. Nascent peptides were produced in the presence of sense transcripts (lanes 1, 3, 5, and 6), but not in the presence of antisense transcripts (lanes 2 and 4). Arrowheads indicate products arising from truncated Cx26 transcripts in all figures.

here and in subsequent figures) are likely to arise from translation from the 0.9-kb transcript in which the 3′-end of the coding region is truncated. Consistent with this, when the two RNAs of different sizes were isolated and used to direct translation individually, proteins of different sizes were generated (our unpublished observations). Furthermore, injection into paired frog oocytes of the 1.1-kb RNA transcript of Cx26 generated functional gap junctions, but injection of the 0.9-kb RNA transcript of Cx26 did not produce intercellular coupling (Suchyna, 1993).

Co-translational Membrane Insertion of Newly Synthesized Cx32 and Cx26

To study the membrane insertion of nascent connexins, RM (derived from canine pancreatic rough endoplasmic reticulum) were added to each translation reaction. The 29-kDa protein from the Cx32 transcript (Figure 1D, lane 5) and the 25-kDa protein from the Cx26 transcript (Figure 1D, lane 6) were also produced in the presence of RM. These proteins are associated with RM and appear to have integrated into membranes because they are resistant to alkaline extraction, which removes peripheral and intra-lumenal proteins.

In addition to the full-length 29-kDa protein, a polypeptide of 27 kDa was also generated from the Cx32 transcript in the presence of RM (Figure 1D, lane 5). The origin of this 27-kDa protein was not definitively established, but could arise from either internal initiation, commonly observed in the in vitro translation system (Zhang and Ling, 1993), inappropriate cleavage by the signal sequence peptidase (as concluded by Falk *et al.*, 1994), or proteolysis at the C-terminus. To distinguish between N-terminal or C-terminal truncation, we translated mRNA templates of Cx32 truncated at the 3′ end by linearization with *Bgl*I. These RNA templates should produce proteins missing 12 amino acids at the C-terminal end of the nascent protein. If the 27-kDa protein was generated due to premature termination or proteolysis at the C-terminal end of the 29-kDa protein, this product will probably be eliminated in translations of the truncated transcript. In contrast, both the 29-kDa and the 27-kDa protein will undergo similar shifts should N-terminal truncation have occurred. Consistent with this latter scenario, translation of the *Bgl*I-truncated transcript of Cx32 generated proteins of ~27 and ~25 kDa (Figure 2, lane 3) compared with proteins of 29 and 27 kDa from the full-length transcript (Figure 2, lane 4).

The pattern of translation products inserting into microsomes from full-length Cx26 transcripts was even more complex (Figure 1D, lane 6). A similar strategy to that used for Cx32 was employed to identify the origin of these lower molecular weight products. Truncated transcripts from a Cx26 template linearized by *Bst*X1 should produce a Cx26 protein missing 51 amino acids at the C-terminal end. This truncation would also remove the potential stem-loop structure at the 3′-end of the template. Consistent with this, only one population of transcripts was produced from this truncated cDNA template (see above discussion in Figure 1) compared with the two cRNA bands produced from the full length template. Translation of this truncated transcript generated only two major protein products of 19 and 16 kDa (Figure 2, lane 1), compared with two major protein products of 25 and 22 kDa and a minor product of ~19 kDa translated from full-length cDNA templates (Figure 2, lane 2). These results suggest that the minor products of ~19 kDa in Figure 2, lane 2, (arrowhead) were probably generated from the 0.9-kb transcript (see Figure 1). The 22-kDa and 25-kDa proteins (Figure 2, lane 2) were likely derived from the 1.1-kb transcript, with the smaller of the two products missing its N-terminal 3 kDa. These results are consistent with the conclusion of Falk *et al.* (1994) that the cell-free system displays inappropriate cleavage of M1 through partial processing at a cryptic site for signal peptidase.

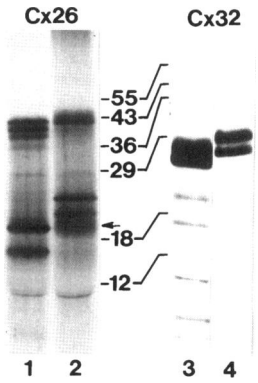

Figure 2. Comparisons of translation products directed by full-length and by truncated transcripts. Full length (lanes 2 and 4) and truncated transcripts (lanes 1 and 3), prepared as described in the text were used to direct translation in rabbit reticulocyte lysate in the presence of RM. Lanes 1 and 2 are Cx26 whereas lanes 3 and 4 are Cx32. In both cases, the major bands were decreased proportionate to the truncation, indicating that these bands arise from loss of N-terminal sequence.

The loss of the N-terminal 3 kDa of both Cx26 and Cx32 could also be caused by other proteases or by internal initiation. The latter is inconsistent with the absence of this truncation in the absence of microsomes (Figure 1D, lanes 1–4) and its observation in connexins lacking appropriate internal initiation signals (Falk *et al.*, 1994). The possibility that other proteases could mediate the truncation was addressed by conducting all translations in the presence of a mixture of protease inhibitors (phenylmethylsulfonyl fluoride or leupeptin, aprotonin, and soybean trypsin inhibitor). No reduction of the cleaved product was observed (our unpublished observations). In addition, after collection of microsomes by spinning at 150,000 $\times$ *g* for 10 min through a 250 mM sucrose cushion, only full length product was found in the supernatant, while the pellet contained both full length and truncated forms (our unpublished observations).

Both Nascent Cx32 and Cx26 in RM Have Native Topological Orientations

The topological structures of the nascent Cx32 and Cx26 in RM membranes were studied by a combination of protease protection and exposure of specific antigenic epitopes. If Cx32 and Cx26 integrated into membranes in their native orientation, they will have an orientation as shown in Figure 3C with both the N-terminal and the C-terminal ends located cytoplasmically. Proteolysis by pronase of the RM vesicles containing nascent Cx32 and Cx26 should generate

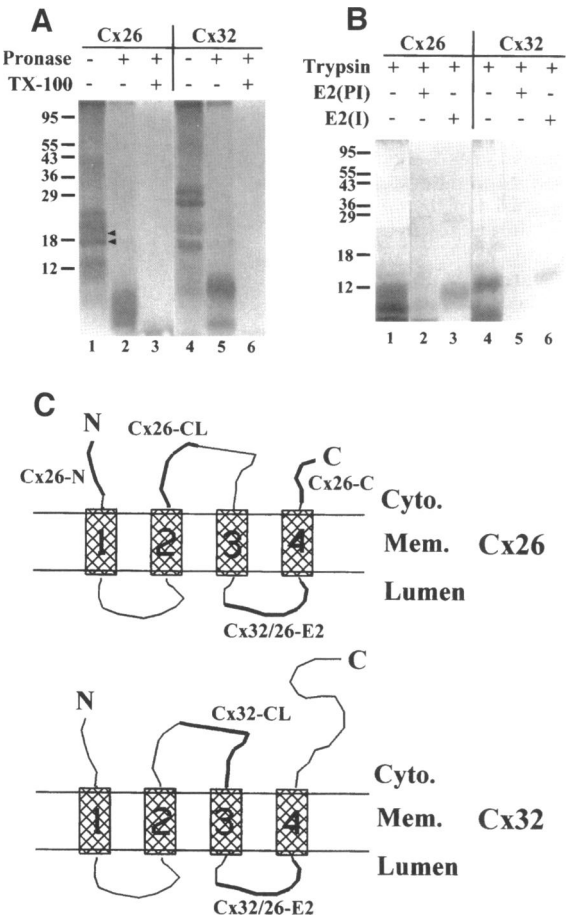

Figure 3. Protease digestion of RM-associated Cx26 and Cx32 in vitro translation products. (A) Pronase digestion of RM-associated Cx26 and Cx32. Membrane-associated translation products Cx26 (lanes 1–3) and Cx32 (lanes 4–6) were treated by pronase (0.1–0.2 mg/ml) in the absence (lanes 2 and 5) or presence (lanes 3 and 6) of 1% Triton X-100. Lanes 1 and 3 are control samples treated without pronase. (B) Trypsin treatment and immunoprecipitation. Membrane-associated translation products Cx26 (lanes 1–3) and Cx32 (lanes 4–6) were treated with trypsin (0.1–0.2 mg/ml). The samples were directly subjected to SDS-PAGE analysis (lanes 1 and 4) or immunoprecipitated with αCx32/Cx26-E2 antibodies (lanes 3 and 6) or with preimmune sera (lanes 2 and 5). (C) Schematic diagram of the membrane topology of Cx32 and Cx26. The membrane topology of Cx26 and Cx32 have been determined from previous studies (see text). The transmembrane segments are depicted as cross-hatched areas. The peptide antibody epitopes are indicated by thick lines. The antigenic sites of the antibodies are as follows: αCx32-CL, amino acid 110–128 of Cx32; αCx32/Cx26-E2, amino acids 166–185 of Cx32; αCx26-N, amino acids 1–17 of Cx26; αCx26-CL, amino acids 101–119 of Cx26; and αCx26-C, amino acids 210–226 of Cx26.

two protected fragments of ~8.4 kDa (N-terminal half: M1-loop-M2 fragment) and ~9.6 kDa (C-terminal half: M3-loop-M4 fragment). Furthermore, an epitope for polyclonal antibody αCx32/Cx26-E2 in the loop linking M3 and M4 segments is located in the RM lumen (Zhang and Nicholson, 1994) and should, therefore, remain intact in the 9.6-kDa protease-resistant fragment (see Figure 3C). All other indicated antibody epitopes in the N- or C-termini or cytoplasmic loops should be removed.

Pronase digestion of membrane fractions of Cx32 translation reactions did, indeed, produce two protease-resistant fragments (10 kDa and 7 kDa; see Figure 3A, lane 5). Trypsin digestion produced a similar pattern (Figure 3B, lane 4). Consistent with the above prediction, only the larger tryptic fragment was immunoprecipitated specifically by αCx32/Cx26-E2 (Figure 3B, lanes 5 and 6).

Poorly resolved peptide fragments of Cx26 in the molecular weight range of 7–9.5 kDa were also protected from pronase digestion (Figure 3A, lane 2). Trypsin digestion of the translation products of Cx26 produced more clearly resolved 9-kDa and 7-kDa fragments (Figure 3B, lane 1). Again only the larger tryptic fragment was immunoprecipitated by αCx32/Cx26-E2 (Figure 3B, lanes 2 and 3), identifying it as being derived from the C-terminal half of Cx26. No protease-resistant fragments were recovered when Triton X-100 was included in the digestion to permeabilize the RM vesicles (Figure 3A, lanes 3 and 6), demonstrating that protease resistance required intact membranes. The slight deviation of the apparent size of the fragments from that predicted is likely due to the nonlinear response of the gel system, particularly in this size range, although the N-terminal truncations of Cx32 and 26 noted above could contribute to smearing of the bands.

We also employed an alternative strategy to more specifically map the exposure of epitopes of Cx32 and 26 to protease treatment in intact or detergent-disrupted microsomes. RM containing co-translationally inserted Cx32 (Figure 4A) or Cx26 (Figure 4B) were incubated with buffer alone or buffer containing 0.1–0.2 mg/ml trypsin to remove antigenic sites exposed extralumenally. After termination of protease action, RM were solubilized in Triton X-100 and the proteins were immunoprecipitated with one of a panel of site-specific polyclonal antibodies (see Figure 3C for epitope locations; see also Zhang and Nicholson, 1994). Antibodies specific to the cytoplasmic loop of Cx32 (αCx32-CL) and the C-terminal cytoplasmic domain of Cx26 (αCx26-C) specifically immunoprecipitated their corresponding translation products in non-protease-treated RM (Figure 4A, lane 3; Figure 4B, lane 4), without cross-reaction (Figure 4A, lane 4; Figure 4B, lane 5). Antibody to the second extracellular domain (αCx32/Cx26-E2) immunoprecipitated both Cx32 and Cx26 translation products (Figure 4, A and B, lane 2). This observation is expected due to the conserved nature of the epitope between Cx32 and Cx26 and is consistent with our observation in Western blots of gap junction isolates (Zhang and Nicholson, 1994). The Cx26-N antibody appears to react

weakly with the nascent Cx26 in these immunoprecipitations (Figure 4B, lane 3). Following proteolysis of the RM, only the αCx32/Cx26-E2 antiserum immunoprecipitated the expected 10-kDa proteolytic fragments from both Cx32 (Figure 4A, lane 5) and Cx26 (Figure 4B, lane 6). All other epitopes were cleaved (Figure 4A, lanes 6 and 7; Figure 4B, lanes 7–9). When the membrane vesicles were permeabilized first with Triton X-100 before addition of trypsin, no protease-resistant fragments reactive to any of the above antibodies were detected (Figure 4A, lanes 8–10; Figure 4B, lanes 10–13), suggesting that the fragment that was immunoprecipitated by αCx32/Cx26-E2 antibody is located in the RM lumen. These results are consistent with our conclusion that both in vitro–translated Cx32 and Cx26 have their native membrane topology.

A final approach to directly assessing the topology of Cx32 and Cx26 in RM that is independent of protease action is the direct immunoprecipitation of intact microsomes with antibodies to epitopes predicted to be cytoplasmic (αCx32-CL or αCx26-CL) or luminal (αCx32/Cx26-E2). Nitrocellulose discs bound with the various antisera were used for affinity binding of the RM membrane vesicles containing Cx32 or Cx26. Luminal epitopes should only be exposed to the antibodies when the RM vesicles are first permeabilized with sonication in the presence of detergent. The results of these binding studies are shown in Table 1 for Cx32 and Table 2 for Cx26. Antibodies directed against the cytoplasmic domains of Cx32 (αCx32-CL) and Cx26 (αCx26-CL) bind their respective intact and permeabilized RM fractions equally. In contrast, αCx32/26-E2 directed against the second extracellular loop of both connexins only binds RM following permeabilization. This result is consistent with the protease digestion study discussed above. Under the same reaction conditions, none of the antibodies used in the binding assay react with a nonrelated nascent membrane protein dipeptide peptidase IV (DPPIV) (Hong and Doyle, 1988) in either intact or solubilized RM fractions.

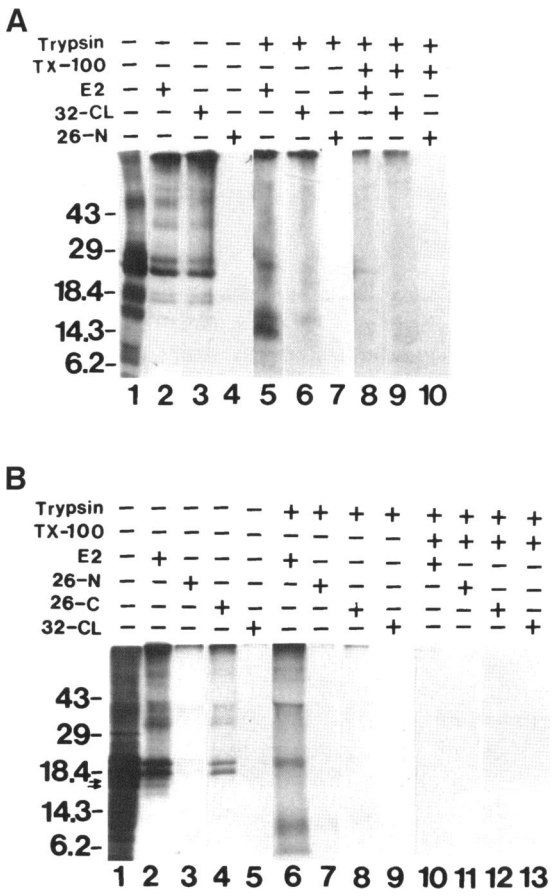

Figure 4. Proteolysis analysis of in vitro–translated and isolated gap junction proteins. (A) Trypsin digestion and immunoprecipitation of in vitro–translated Cx32. Membrane-associated Cx32 was treated without (lanes 1–4) or with trypsin in the absence (lanes 5–7) or presence (lanes 8–10) of Triton X-100. Immunoprecipitation of trypsinized or untreated samples was performed with αCx32/Cx26-E2 (lanes 2, 5, and 8), αCx32-CL (lanes 3, 6, and 9), or αCx26-N as a negative control (lanes 4, 7, and 10). (B) Trypsin digestion and immunoprecipitation of in vitro–translated Cx26. Membrane-associated Cx26 was treated without (lanes 1–5) or with trypsin in the absence (lanes 6–9) or presence (lanes 10–13) of Triton X-100. Immunoprecipitation of trypsinized or untreated samples was performed with αCx32/Cx26-E2 (lanes 2, 6, and 10), αCx26-N (lanes 3, 7, and 10), αCx26-C (lanes 4, 8, and 11), or αCx32-CL as a negative control (lanes 5, 9, and 13).

Post-translational Membrane Insertion of Nascent Cx26

We next examined whether Cx32 and Cx26 can insert into membranes post-translationally. In this study, the translation of Cx32 and Cx26 was completed in rabbit reticulocyte lysate in the absence of RM, followed by RNase A treatment to stop translation by removing all RNA templates. In some experiments, puromycin was also added to ensure release of the polypeptide from the ribosome but these results did not differ from RNase treatment alone. Microsomes were then added to the translation reaction mixture and incubated for 90 min at 30°C after which the microsomes were recovered and analyzed as described above.

Under these conditions, translation products of Cx26 were found to be associated with the post-translationally added RM (Figure 5A, lane 4) whereas the translation products of Cx32 were not (Figure 5A, lane 2). In a parallel experiment, the same Cx32 and Cx26 transcripts were shown to direct co-translational insertion of the respective proteins into RM (Figure 5A, lanes 1 and 3, respectively). The post-translational insertion of Cx26

Table 1. Immunoprecipitation of Cx32 in microsomes

	Cx32				DPP IV			
	Intact RM		Disrupted RM		Intact RM		Disrupted RM	
Antibodies[a]	Cx32-CL	-E2	Cx32-CL	-E2	Cx32-CL	-E2	Cx32-CL	-E2
Binding[b]	1.75	1.06	1.61	1.52	1.09	1.08	1.14	1.13
n	9	9	9	9	9	9	9	10
p	<0.005	>0.005	<0.005	<0.025	>0.005	>0.005	>0.005	>0.005

[a] The antibodies used are αCx32-CL and αCx32/Cx26-E2.

[b] The numbers represent the fold increase of radioactivity bound to the discs over background.

seemed to favor the full length product (Figure 5A, compare lanes 3 and 4). Like their co-translationally inserted counterpart, post-translationally inserted Cx26 proteins are also resistant to alkaline extraction, suggesting that they are integrated into the membrane. This was further demonstrated by the failure to recover connexins in the pellet in the absence of membranes (see Figure 7, lane 2).

Genuine post-translational insertion of membrane proteins is believed to function independent of the SRP/docking protein complex. We tested this directly by repeating the above experiment using *N*-ethylmaleimide (NEM)-treated RM. It has been shown that the NEM treatment inactivates the membrane-associated receptors of SRP (Gilmore *et al.*, 1982) and prevents the normal co-translational insertion of membrane proteins. Consistent with this, the co-translational membrane insertion of Cx32 was completely prevented by NEM treatment (Figure 5B, compare lanes 1 and 2). By contrast, NEM treatment only slightly reduced the post-translational membrane insertion of full length Cx26. By contrast, the "apparent" post-translational insertion of the lower molecular weight products resulting from incomplete RNase treatment before microsome addition was eliminated by NEM treatment (Figure 5B, compare lanes 3 and 4). This is consistent with the smaller products representing polypeptides that were not released from the ribosomes by RNase treatment and could thus still utilize an SRP-dependent mechanism linked to potential cryptic cleavage by signal peptidase. The SRP independence of Cx26 post-translational insertion was further indicated by similar results with wheat germ extract, which does not contain an SRP compatible with mammalian translocation machinery, yet can still support post-translational insertion of Cx26 (our unpublished observations).

To determine the topological membrane orientation of post-translationally inserted Cx26 proteins, we performed a proteolysis/membrane protein assay. Two fragments were protected from V8 digestion of the post-translationally inserted Cx26 proteins (Figure 5C, lane 2). These two protease-resistant fragments are identical to those produced from co-translationally inserted Cx26 (Figure 5C, lane 1) and correspond in size to the N-terminal (MI-loop-M2) and C-terminal (M3-loop-M4) fragments derived from Cx26 by similar proteolysis of isolated gap junctions (Zhang and Nicholson, 1994). As expected, when protease treatment is preceded by Triton X-100, no fragments are pelleted.

Table 2. Immunoprecipitation of Cx26 in microsomes

	Cx26				DPP IV			
	Intact RM		Disrupted RM		Intact RM		Disrupted RM	
Antibodies[a]	Cx26-CL	-E2	Cx26-CL	-E2	Cx26-CL	-E2	Cx26-CL	-E2
Binding[b]	1.83	1.03	1.46	1.58	0.97	0.95	1.00	1.10
n	11	9	9	9	12	9	9	9
p	<0.025	>0.005	<0.025	<0.025	>0.005	>0.005	>0.005	>0.005

[a] The antibodies used are αCx26-CL and αCx32/Cx26-E2.

[b] The numbers represent the fold increase of radioactivity bound to the discs over background.

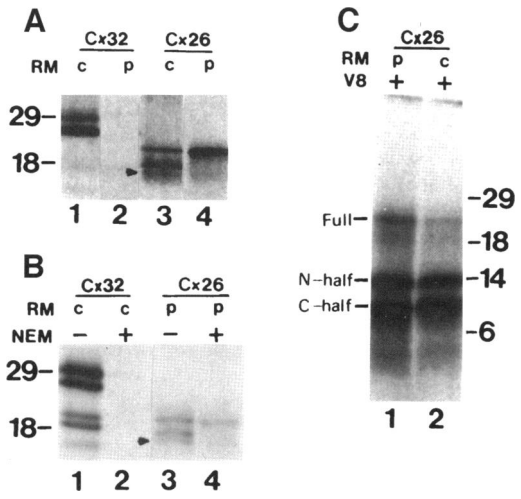

Figure 5. Post-translational membrane insertion of in vitro–translated Cx32 and Cx26. (A) Cx26 can be inserted in RM membrane post-translationally. RM was added post-translationally to the translation reaction directed by Cx32 (lane 2) and Cx26 (lane 4) transcripts. Only the translation products of Cx26 can insert into RM post-translationally (lane 4). Lanes 1 and 3 show the co-translationally inserted Cx32 (lane 1) and Cx26 (lane 3). (B) The post-translational membrane insertion of Cx26 does not depend on a SRP-mediated mechanism. RM was treated by NEM to deactivate the SRP-receptor before it was added to the lysate co-translationally for Cx32 (lane 2) or post-translationally for Cx26 (lane 4). Normal RM was used in lanes 1 and 3 as controls. (C) Post-translationally inserted Cx26 has the same protease digestion pattern as co-translationally inserted Cx26. Cx26-associated with RM by either a co-translational (lane 1) or post-translational (lane 2) mechanism were treated with V8 protease. Both N- and C-terminal halves were generated from both reactions. c, co-translational; p, post-translational.

The Post-translational Membrane Insertion of Cx26 Requires Ribonucleotide Triphosphate

To determine the cofactor requirements for the post-translational membrane insertion of Cx26, we performed a complementation study. Following the synthesis of Cx26 in rabbit reticulocyte lysate in the absence of RM, RNA templates were removed by RNase A digestion. The translation mixture was then stripped of low molecular weight components by collecting the excluded volumes of two successive Sephadex G-25 spin columns. The collected fraction was then divided into equal aliquots and supplemented with RM and different concentrations of ATP or other cofactors. This ensured equal loadings of translated product in the comparisons shown in Figure 6, A–C. Following a 90-min incubation at 30°C, membrane insertion was assessed by Na_2CO_3-resistant association with the microsomal pellet. As shown in Figure 6A, significant post-translational membrane insertion of Cx26 required at least 5 mM ATP (Figure 6A, lane 3) and increased with concentration up to 20 mM. Two non-hydrolyzable ATP analogues, ATPγS and AMP-PCP, also support the post-translational membrane insertion of Cx26 (Figure 6B, lanes 4 and 5), suggesting that hydrolysis of ATP is not required in the post-translational membrane insertion of Cx26 (see DISCUSSION). Similar concentrations of PPi (Figure 6B, lane 6), ADP (Figure 6B, lane 7), and AMP (Figure 6B, lane 8) failed to promote the post-translational insertion, ruling out the possibility of potential contamination of ATP by these degradation products. Surprisingly, UTP, GTP, or CTP can also support the post-translational membrane insertion of Cx26 with only slightly reduced potency compared with ATP, as assessed at 5 mM and 0.5 mM concentrations (Figure 6C).

The Post-translational Membrane Insertion of Cx26 Is Determined by Its Internal Amino Acid Sequences

We have shown that Cx32, unlike Cx26, does not insert into RM post-translationally (Figure 5) despite an overall 64% amino acid identity between Cx32 and Cx26 (Zhang and Nicholson, 1989). A major difference between these two proteins is the length of the cytoplasmic tail and hence their overall hydrophilicity. To test whether the lack of this hydrophilic domain in

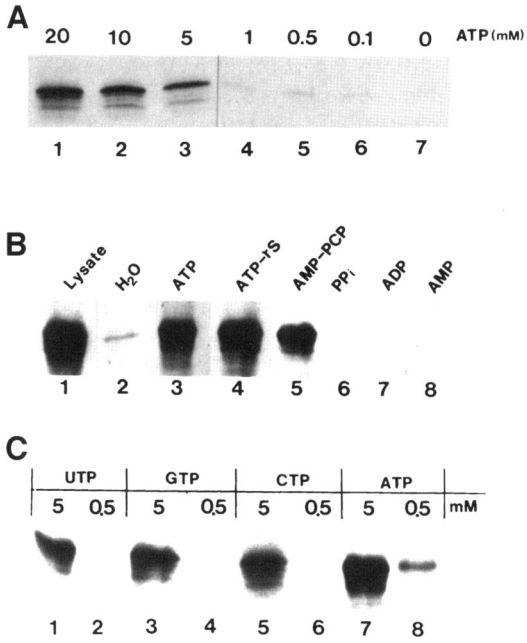

Figure 6. The post-translational membrane insertion of Cx26 is ribonucleotide dependent. Cx26 transcript was used to direct translation in the absence of RM. Before RM were added post-translationally to the reaction, the lysate mixture was stripped of small molecular weight component (see MATERIALS AND METHODS) and then complemented with different concentrations of ATP (A), or nonhydrolyzable ATP analogues, PPi, ADP, or AMP at 5 mM each (B), or different concentrations of UTP, GTP, or CTP (C). All four ribonucleotides at 5mM concentration (ATP at a slightly lower level) and nonhydrolyzable ATP analogues can support the post-translational membrane insertion of Cx26.

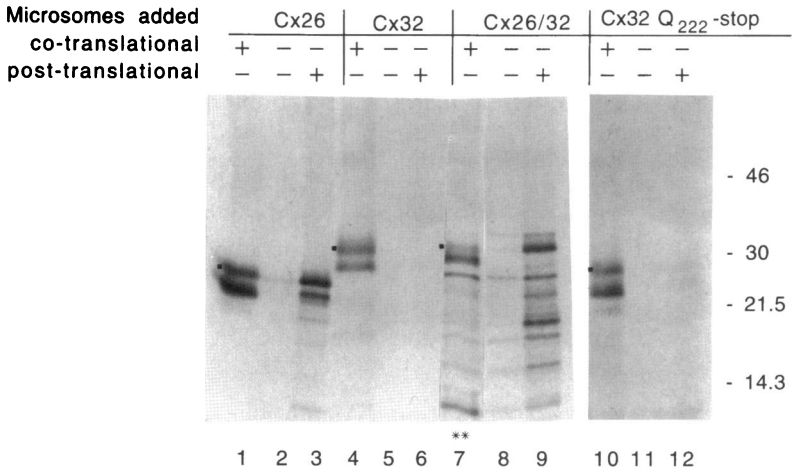

Figure 7. The ability of Cx26 to insert into microsomal membranes post-translationally is not due to the length of its carboxy-terminal tail. Four different constructs were translated in the presence or absence of microsomes: Cx26 *wt*, Cx32 *wt*, $Cx26_{(1-199)}/32_{(200-283)}$ (Cx26/32), and Cx32 Q_{222}-stop. For each construct tested, the first lane shows the results of a co-translational insertion into microsomes with the full length product marked with a square. The second lane represents a translation with no microsomes added to control for nonspecific aggregation products being pelleted. The third lane represents the results of the post-translational insertion. Where microsomes were only added after translation was terminated, competence for post-translation insertion was unique to Cx26 and was unaffected in a chimera where the C-terminal domain was replaced by the substantially longer region of Cx32 (Cx26/32). Conversely, the inability of Cx32 to insert post-translationally was unaffected by a truncation of the C-terminal domain to a length comparable to that of Cx26. It is notable that post-translational insertion (of both Cx26 and Cx26/32) favored the full length product (see text). The translation of Cx26/32 showed some protein products smaller than the predicted molecular weight. We believe these smaller products result from proteolysis of inappropriately folded translation product in the lysate before insertion. **To equalize protein loadings, we show a longer exposure in this lane.

Cx26 is responsible for its unique properties, we engineered both a Cx32 construct truncated to the length of Cx26 by insertion of a stop codon at position 222, and a chimeric Cx26 fused with the carboxy terminal tail of Cx32. The $Cx26_{1-199}/Cx32_{200-283}$ chimera retained the ability to insert into RM post-translationally (Figure 7, lanes 7–9), like the parental Cx26 (Figure 7, lanes 1–3). In contrast, the truncated Cx32 (Figure 7, lanes 10–12) behaved like full length Cx32 (Figure 7, lanes 4–6), inserting only co-translationally. These results suggest that the capacity of Cx26 for post-translational membrane insertion is not determined by overall length or hydrophobicity, but by specific sequences in Cx26 to the N-terminal side of residue 199.

As noted above, post-translational insertion results in enrichment of the full length product over the product truncated by ~2 kDa. This is consistent with the proposed role of cryptic signal peptidase cleavage in this truncation (Falk *et al.*, 1993), as one might expect that SRP-independent post-translational insertion may not use the same signal peptidase–associated machinery of co-translational insertion. The large number of substantially lower products seen in translations of the chimeric protein appear to reflect increased proteolysis, perhaps due to inadequate folding of the chimeria. The number and level of these products could be reduced by protease inhibitors, but only at the cost of translational efficiency. More proteolysis was evident in post-translational samples where the protein is exposed longer to the lysate before insertion into the membrane.

DISCUSSION

In this study, we have demonstrated that both Cx32 and Cx26 can be synthesized in an in vitro translation system. Both nascent Cx32 and Cx26 translocated into dog pancreatic RM co-translationally. These nascent molecules in RM have a topological structure indistinguishable from that in isolated gap junctions (Zhang and Nicholson, 1994).

The topology of the connexins were established using a proteolysis/membrane protection assay that produced two protected fragments from both Cx32 and 26 (Figure 3) that corresponded in size to those in proteolysed junctional fractions from mouse liver (Nicholson *et al.*, 1987; Zhang and Nicholson, 1994). Specific sites were also demonstrated to be disposed on the appropriate side of the membranes by using immunoprecipitation of the proteins from intact or lysed RM, before or after proteolysis, with a panel of site-specific antibodies to cytoplasmic and lumenal domains of the connexins. Within the resolution of each of these assays, all of the protein inserted into microsomes had a "native" topology. Concurrent studies by Falk *et al.* (1994) had produced equivocal results in this regard, in which antibodies against specific epitopes suggested that an inappropriate topology was produced in the microsomes.

In many of the translation reactions studied, multiple products of translation were evident. Some are consistent with the tendency of both Cx32 and Cx26 to aggregate into dimers in SDS-PAGE. However, most were shorter products that appear to represent a combination of internal initiation, proteolysis, and in the case of Cx26, products of a shorter transcript, marked on all figures with an arrowhead. Additional bands arose on addition of RM, which appear to represent a signal peptidase activity in the RM that inappropriately recognizes a cryptic cleavage site at the C-terminal end

of M1. This is consistent with the results of Falk *et al.* (1994) who demonstrated this to be a common result in several members of the connexin family. We have observed this property for Cx32, Cx26, and Cx43. Although this is likely to be an artifact of the cell-free system, a similar pattern of cleavage has also been seen in transfected cells that overexpress connexins (Falk *et al.*, 1994).

Surprisingly, we also found that Cx26 can insert into RM post-translationally. The detailed pathway of this process is not known, although our results indicate that an SRP-mediated process is not involved, as insertion is resistant to NEM pre-treatment of the microsomes. This ensures that such post-translational insertion could not arise from residual polypeptides associated with the ribosome following RNase treatment that could still utilize the co-translational machinery. This was also confirmed in some experiments by the use of puromycin treatment in addition to RNAse before the addition of RM (our own unpublished observations). Finally, it should also be noted that post-translationally inserted products did not include significant amounts of the truncated product, proposed to result from cryptic signal peptidase cleavage. This is also consistent with the independence of the post-translational mechanism on SRP and, presumably, the associated Sec61 and signal peptidase complex. Interestingly, the shorter product arising from translation of the truncated message also fails to insert post-translationally, indicating that the intact protein may be required for this process.

The post-translational insertion of Cx26 is highly unusual for a polytopic plasma membrane protein from higher eukaryotes. Human glucose transporter has been shown to insert into membranes post-translationally (Mueckler and Lodish, 1986a,b), but with an efficiency much lower than seen here for connexins. Post-translational membrane insertion has also been found in association with other native or mutant non-polytopic membrane proteins, for instance, yeast pre-pro-α-factor (Hansen *et al.*, 1986; Rothblatt and Meyer, 1986; Waters *et al.*, 1986), a fusion protein of lactamase and chimpanzee α globin (Perara *et al.*, 1986), and bovine preprolactin (Connolly and Gilmore, 1986). In all these cases, post-translational insertion is dependent on ATP-hydrolysis, a property that has usually been taken to suggest the role of a chaperone protein in this process (Flynn *et al.*, 1989; Martin *et al.*, 1992; Frydman *et al.*, 1994). The post-translational membrane insertion of Cx26 also requires ATP, but in this case its hydrolysis is not required, and the specificity for nucleotide is low. This feature is unique among published examples of post-translational translocation of membrane proteins.

The specificity of the post-translational membrane insertion of Cx26 is perhaps best illustrated by the failure of the homologous Cx32 to display the same property, despite 64% sequence identity. Chimeras of Cx32 and Cx26 indicate that it is not gross hydrophobicity or length that are important, but specific sequences within Cx26. Whether these determinants lie within the membrane or in the more variable cytoplasmic domains will require a more extensive analysis. Identification of the machinery involved in this process is likely to be of great relevance to our understanding of translocation of membrane proteins in general. In particular, it may provide a window into the early evolutionary transition from post-translational to almost exclusively co-translational membrane translocation of polypeptides. Its relevance to in vivo models of gap junctional assembly is more obscure. There is no evidence for or against a significant role for post-translational insertion in situ. Should it occur, it could provide a means to separate connexin populations during biosynthesis, thereby limiting the formation of mixed oligomers.

Of more immediate relevance is the potential value of this technique as a means for reconstituting the gap junction hemichannel directly from RNA, potentially providing an exceptionally well defined system for in vitro study of the protein, and the reconstitution of mutant variants of connexins. Given the extensive topological characterization, it also provides one of the best available models for studying insertion of a polytopic membrane protein.

ACKNOWLEDGMENTS

The authors thank Feng Gao for her technical assistance throughout this project, and Tom Rapoport and Bernard Dobberstein for valuable scientific input. The work was supported by National Institutes of Health grants CA-48049 and HL-48773, and a Scholars Award from the Pew Charitable Trust. B.J.N. is an American Heart Association Established Investigator.

REFERENCES

Andrews, D. (1989). Examining protein translocation in cell-free systems and microinjected *Xenopus* oocytes. Biotechnology *7*, 960–967.

Bennett, M.V.L., and Goodenough, D.A. (1978). Gap junctions, electronic coupling and intercellular communication. Neurol. Res. Prog. Bull. *16*, 373–486.

Connolly, T., and Gilmore, R. (1986). Formation of a functional ribosome-membrane junction during translocation requires the participation of a GTP-binding protein. J. Cell Biol. *103*, 2253–2261.

Evans, E.A., Gilmore, R., and Blobel, G. (1986). Purification of microsomal signal peptidase as a complex. Proc. Natl. Acad. Sci. USA *83*, 581–585.

Falk, M.M., Kumar, N.M., and Gilula, N.B. (1994). Membrane insertion of gap junction connexins: polytopic channel forming membrane proteins. J. Cell Biol. *127*, 343–355.

Flynn, G.C., Chappell, T.G., and Rothman, J.E. (1989). Peptide binding and release by proteins implicated as catalysts of protein assembly. Science *245*, 385–390.

Frydman, J., Nimmesgern, E., Ohtsuka, K., and Hartl, F.U. (1994). Folding of nascent polypeptide chains in a high molecular mass assembly with molecular chaperones. Nature *370*, 111–117.

Gilmore, R., Blobel, G., and Walter, P. (1982). Protein translocation across the endoplasmic reticulum. I. Detection in the microsomal

membrane of a receptor for the signal recognition particle. J. Cell Biol. *95*, 463–469.

Guthrie, S.C., and Gilula, N.B. (1989). Gap junctional communication and development. Trends Neurosci. *12*, 12–16.

Hansen, W., Garcia, P.D., and Walter, P. (1986). In vitro protein translocation across the yeast endoplasmic reticulum: ATP-dependent post-translational translocation of the prepro-α-factor. Cell *45*, 397–406.

Hertzberg, E.L., Disher, R.M., Tiller, A.A., Zhou, Y., Cooke, R.G. (1988). Topology of the M_r27,000 liver gap junction protein: cytoplasmic localization of amino- and carboxy-termini and a hydrophilic domain which is protease sensitive. J. Biol. Chem. *263*, 19105–19111.

Hong, W., and Doyle, D. (1988). Membrane orientation of rat gp110 as studied by in vitro translation. J. Biol. Chem. *263*, 16892–16898.

Jagus, R. (1987). Translation in cell-free systems. Methods Enzymol. *12*, 267–276.

Klaunig, J.E., and Ruch, R.J. (1990). Biology of disease: role of inhibition of intercellular communication in carcinogenesis. Lab Invest. *62*, 135–146.

Kumar, N.R., and Gilula, N.B. (1992). Molecular biology and genetics of gap junction channels. Semin. Cell Biol. *3*, 3–16.

Kunkel, T.A., Roberts, J.D., and Zakour, R.A. (1987). Rapid and effective site-specific mutagenesis without phenotypic selection. Methods Enzymol. *154*, 367–382.

Laemmli, U.K. (1970). Cleavage of structural proteins during the assembly of the head of the bacteriophage T4. Nature *227*, 680–685.

Loewenstein, W.R. (1979). Junctional intercellular communication and the control of cell growth. Biochim. Biophys. Acta *560*, 1–65.

Martin, J., Horwich, A.L., and Hartl, F.U. (1992). Prevention of protein denaturation under heat stress by the chaperonin Hsp60. Science *258*, 995–998.

Meyer, D.I., Krause, E., and Dobberstein, B. (1982). Secretory protein translocation across membrane: the role of the "docking protein." Nature *297*, 647–650.

Milks, L.C., Kumar, N.M., Houghten, R., Unwin, N., and Gilula, N. (1988). Topology of the 32 kD liver gap junction protein determined by site-directed antibody localizations. EMBO J. *7*, 2967–2975.

Mueckler, M., and Lodish, H.F. (1986a). The human glucose transporter can insert post-translationally into microsomes. Cell *44*, 629–637.

Mueckler, M., and Lodish, H.F. (1986b). Post-translational insertion of a fragment of the glucose transporter into microsomes requires phosphoanhydride bond cleavage. Nature *322*, 549–552.

Musil, L.S., and Goodenough, D.A. (1993). Multisubunit assembly of an integral plasma membrane channel protein, gap junction connexin 43, occurs after exit from the ER. Cell *74*, 1065–1077.

Nicholson, B.J., Dermietzel, R., Teplow, D., Traub, O., Willecke, K., and Revel, J.-P. (1987). Two homologous proteins of hepatic gap junctions. Nature *329*, 732–734.

Nicholson, B.J., Hunkapiller, M.W., Grim, L.B., Hood, L.E., and Revel, J.P. (1981). Rat liver gap junction protein: properties and partial sequence. Proc. Natl. Acad. Sci. USA *78*, 7594–7598.

Paul, D.L. (1986). Molecular cloning of cDNA for rat liver gap junctional protein. J. Cell Biol. *103*, 123–134.

Perara, E., Rothman, R.E., and Lingappa, V.R. (1986). Uncoupling translocation from translation: implications for transport of proteins across membranes. Science *232*, 348–352.

Rahman, S., and Evans, W.H. (1991). Topography of connexin 32 in rat liver gap junctions: evidence for an intramolecular disulfide linkage connecting the two extracellular loops. J. Cell Sci. *100*, 567-578.

Rothblatt, J.A., and Meyer, D.I. (1986). Secretion in yeast: translocation and glycosylation of prepro-α factor in vitro can occur via an ATP-dependent post-translational mechanism. EMBO J. *5*, 1031–1036.

Rothman, R.E., Andrews, D.W., Calayag, M.C., and Lingappa, V.R. (1988). Construction of defined polytopic integral transmembrane proteins. J. Biol. Chem. *263*, 10470–10480.

Sheridan, J.D., and Atkinson, M.M. (1985). Physiological roles of permeable junctions: some possibilities. Annu. Rev. Physiol. *47*, 337–353.

Spray, D.C., and Burt, J.M. (1990). Structure-activity relations of the cardiac gap junction channel. Am. J. Physiol. *258*, C195–C205.

Suchyna T.M. (1993). The properties and mechanism of gap junction channel voltage gating. Ph.D. Thesis. Buffalo, NY: State University of New York.

von Heijne, G., and Gavel, Y. (1988). Topogenic signals in integral membrane proteins. Eur. J. Biochem. *174*, 671–678.

Walter, P., and Blobel, G. (1980). Purification of a membrane-associated protein complex required for protein translocation across the endoplasmic reticulum. Proc. Natl. Acad. Sci. USA *77*, 7112–7116.

Waters, M.G., Chirico, W.J., and Blobel, G. (1986). Protein translocation across the yeast microsomal membrane is stimulated by a soluble factor. J. Cell Biol. *103*, 2629–2636.

Yancey, S.B., John, S.A., Lal, R., Austin, B.J., and Revel, J.-P. (1989). The 43 kD polypeptide of heart gap junctions: immunolocalization, topology and functional domains. J. Cell Biol. *108*, 2241–2254.

Yang, X.-D., Korn, H., and Faber, D.S. (1990). Long-term potentiation of electronic coupling as mixed synapses. Nature *348*, 542–545.

Zhang, J.T., Lee, C.-H., Duthie, M., and Ling, V. (1995). Topological determinants of internal transmembrane segments in P-glycoprotein sequences. J. Biol. Chem. *270*, 1742–1746.

Zhang, J.T., and Ling, V. (1991). Study of membrane orientation and glycosylated extracellular loops of mouse P-glycoprotein by in vitro translation. J. Biol. Chem. *266*, 18224–18232.

Zhang, J.T., and Ling, V. (1993). Membrane orientation of transmembrane segments 11 and 12 of MDR- and non-MDR-associated P-glycoproteins. Biochim. Biophys. Acta *1153*, 191–202.

Zhang, J.T., and Nicholson, B.J. (1989). Sequence and tissue distribution of a second protein of hepatic gap junctions, Cx26, as deduced from its cDNA. J. Cell Biol. *109*, 3391–3410.

Zhang, J.T., and Nicholson, B.J. (1994). The topological structure of connexin 26 and its distribution compared to connexin 32 in hepatic gap junctions. J. Membr. Biol. *139*, 15–29.